Supplementary Information

(A.W. Snow, G.G. Jernigan and M.G. Ancona, "Packing Density of $HS(CH_2)_nCOOH$ self-assembled monolayers)

Effective (n_{eff}) and Stoichiometric (n_{chain}) Numbers of Atoms in SAM Molecular Structure.

Determination of this n_{eff} parameter was developed as part of a procedure to assess packing density metric for bidentate and tridentate alkanethiol SAMs by T.R. Lee et al.[1] It is based on the relation between the attenuation of substrate emission intensity and the thickness, or extended chain length, for a homologous series of normal alkanethiol SAMS. This relation was derived by Bain and Whitesides[2] and is defined by Eqn. 2 in the main text as:

$$\ln(I) = \ln(I_0) - \frac{d}{\lambda \sin \theta}$$

where I is the intensity of emitted electrons from the surface, I_o is the intensity of emitted electrons without attenuation, d is the thickness of the solid attenuating the emitted electrons, θ is the angle the emitted electrons escape the surface with respect to the electron detector, and λ is the attenuation length. For an extended chain morphology with all chains at a common tilt angle, the SAM film thickness d may be equated to the sum of thickness contributions of the sulfur, methylene and methyl groups (i.e. $d = d_S + (n\text{-}1)d_{CH2} + d_{CH3}$ where n is the number of carbon atoms in the normal alkanethiol molecule). If the methyl contribution is assumed to be equal to that for the methylene group, and that for the sulfur presumed to be 1.5x that of the methylene group, $d = d_{CH2}(n + 1.5)$. For an Au substrate the above equation may be recast as follows:

$$\ln(I_{Au}) = \ln(I_0) - \left(\frac{d_{CH2}}{\lambda \sin \theta} \right)(n + 1.5)$$

A plot of $\ln(I_{Au})$ vs $(n + 1.5)$ is linear with the slope relating to attenuation determining parameters of the SAM and measurement takeoff angle. This plot with a linear fit for the $CH_3(CH_2)_5SH$, $CH_3(CH_2)_{10}SH$ and $CH_3(CH_2)_{15}SH$ SAMs of the current study is presented in Fig. S1. The corresponding stoichiometric chain length parameter, n_{chain}, includes the methylene and methyl carbon atoms but not sulfur, and for the members of this series the respective values are 6, 11 and 16. The n_{eff} values entered in Table 3 of the main text determined simply reflect the small departure of the data from the linear fit. By assuming that the SAM/substrate material parameters and the XPS instrument parameters reflected in the slope and intercept of the Fig. S1 plot are also applicable to the –COOH terminated SAMs, this plot may be used to determine values of n_{eff} for those depositions. In this case the two oxygen atoms in the terminal group are assumed to have attenuating effects equivalent to carbon on the Au substrate emission as has been assumed for other SAM systems.[3] The n_{eff} parameter for a particular –COOH terminated SAM is determined by inserting the corresponding $\ln(I_{Au})$ measurement into the linear fit equation and solving for *n*. The n_{eff} values for direct, acetic-acid-assisted and butyl-amine-assisted depositions at each chain length are spotted on the Fig. S1 plot of the linear fit equation. For each group of chain lengths the order of increasing attenuation (and increasing n_{eff}) is acetic-acid-assisted < butyl-amine-assisted < direct deposition. In the determination of the nchain parameter, the oxygen atoms are counted as carbon equivalents which adds 3 from the –COOH terminal group to the methylene count although both oxygen atoms cannot be strictly considered as part of a linear chain.

Comparison of XPS Theoretical Modeling and Experimental Data.

The XPS characterization data and modeling of the SAMs produced by the three deposition methods are graphically summarized are graphically summarized in Fig. S2. With

regard to a morphology of the $HS(CH_2)_nCOOH$ SAMs, our interpretation is that there is a density

of sulfur bonding to the substrate that is less than the 1 in 3 Au surface atoms which is reported

for perfectly ordered alkanethiol SAMs and on which our modeling results are based. The

vertical displacement of the modeling curves above the experimental curves results from this

Au-bonded bound sulfur density and forms the basis of the calculated packing fractions via

modeling given in Table 3. Within the three SAM deposition conditions, it appears that the

butyl-amine-assisted deposition is the least effective in achieving a high density of bound sulfur

and, conversely, results in more free thiol adsorbed to the SAM surface as indicated in Fig. S2a.

The methylene chains are more extended than coiled with the exception of the shortest chain

length member. The slope for the plot of the random coil model in Fig. S2b reflects this result

pertaining to the molecular shape. The slopes of the extended chain models conform well with

the experimental result. The near constant $C1s(CO_2)$ emission intensity as a function of chain

length in Fig. S2c indicates terminal -COOH group is mostly situated at the air interface of the

SAM rather than submerged significantly below the surface. The slight downward curvature

may be a consequence of a variable amount of physisorbed layer on the SAM that would cause a

slight attenuation of this emission. This physisorbed partial layer would correlate with the

$S2p(SH)$ emission in Fig. S2a. The vertical order of the $C1s(CO_2)$ curves in Fig. S2c indicates

that the direct deposition deposits the largest quantity of -COOH functionality, however this

deposition also results in the largest quantity of partial physisorption as indicated by its large Au

substrate attenuation result in Fig. 4a of the main text. The physisorption of $HS(CH_2)_nCOOH$

molecules on $HS(CH_2)_nCOOH$ SAMs is an issue that has not been resolved in the literature. It is

reasonably well-known that good solvent rinsing of the substrate after SAM formation is

necessary to remove physisorbed SAM molecules whether they be simple alkanethiol or

functionalized alkanethiols. For this $HS(CH_2)_nCOOH$ SAM system, some reports claim physisorbed $HS(CH_2)_nCOOH$ is removable[4-5] while others claim that it is not removable.[6-9] In our experience, double washing with ethanol, 10% acetic in ethanol or 10% butyl amine in ethanol did not effect a complete removal. In further appreciation of this difficulty, an experiment was conducted where an acetic-acid-assisted $HS(CH_2)_{15}COOH$ SAM preparation, including 2x washings with 10% acetic acid/ethanol and 100% ethanol, was immersed in a 0.02 mM $HS(CH_2)_{15}COOH$/ethanol solution followed again by 2x ethanol immersion washings and then XPS analysis. The Table 1 $HS(CH_2)_{15}COOH$ HAc assisted SAM XPS peak areas changed as follows: Au4f (55507→36000); S2p(430→488); C1sCO$_2$(595→601); C1sCH$_2$(6677→6920). This experiment, using a SAM deposition procedure designed to reduce physisorbed layer formation during its formation, resulted in significant increases in carbon and sulfur peak areas and in much larger gold attenuation when the acetic acid was absent in a second 0.02 mM $HS(CH_2)_{15}COOH$/ethanol immersion. This additional physisorption was not removable by simple solvent washing. If a procedure is claimed to be successful for removal of physisorbed $HS(CH_2)_nCOOH$ from SAMs of this type, it should be documented in detail.

C1s(CO$_2$) Emission Maximum Shift.

As indicated in the discussion of packing density dependence on SAM deposition method, the C1s(CO$_2$) peak emission has a larger variation in binding energy with chain length than does the C1s(CH$_2$) emission. This peaks binding energy dependence on deposition conditions as a function of chain length is plotted Fig. S3 and offers additional insight towards the morphology of the deposited SAM. The direct deposition, the acetic-acid-assisted deposition and comparable results from a recent report[5] display a near linear increase in C1s(CO$_2$) peak

maximum binding energy with increasing chain length. This is consistent with the –COOH groups located at the air interface of the SAM and progressively getting further from the metal substrate as the chain length increases. The near independence of C1s(CO_2) peak intensity on chain length (Fig. S2c) discussed above complements this morphology. However the butyl-amine-assisted deposition deviates from this behavior in both plots. As such, it represents the most disordered and least dense SAM. The ammonium carboxylate ion pair molecular state during SAM formation correlates with this effect. It is also interesting to note the vertical displacement in binding energy of the near linear plots in Fig. S3 for the direct deposition, acetic-acid-assisted deposition and data from Ref 5. The descending order is acetic-acid-assisted deposition > Ref 5 > direct deposition. As discussed in the preceding paragraph, the higher binding energies correlate with the thicker direct deposition SAMs. As depicted in Table 3, the direct deposition is a partial multilayer. The deposition of Ref 5 is also a form of a direct deposition with sonication used in the washing after SAM formation. The acetic-acid-assisted deposition more closely approaches a single monolayer.

References.

1. J.-S. Park, A. N. Vo, D. Barriet, Y.-S. Shon and T.R. Lee, *Langmuir,* 2005, **21**, 2902.

2. C. D. Bain and G. M. Whitesides, *J. Phys. Chem.*, 1989, **93**, 1670.

3. P. Harder, M. Brunze, R. Dahint, G. M. Whitesides and P. E. Laibinis, *J. Phys. Chem. B*, 1998, **102**, 426.

4. S. M. Mendoza, I. Arfaoui, S. Zanarini, F. Paolucci and P. Rudolf, *Langmuir*, 2007, **23**, 582.

5. S. D. Techane, L. J. Gamble, D. G. Castner, *J. Phys. Chem. C*, 2011, **115**, 9432.

6. E. Ito, K. Konno, J. Noh, K. Kanai, Y. Ouchi, K. Seki and M. Hara, *Appl. Surf. Sci*. 2005, **244**, 584.

7. R. Arnold, W. Azzam, A. Terfort and C. Wöll, *Langmuir*, 2002, **18**, 3980.

8. T. M. Willey, A. L. Vance, T. van Buuren, C. Bostedt, A. J. Nelson, L. J. Terminello and C. S. Fadley, *Langmuir*, 2004, **20**, 2746.

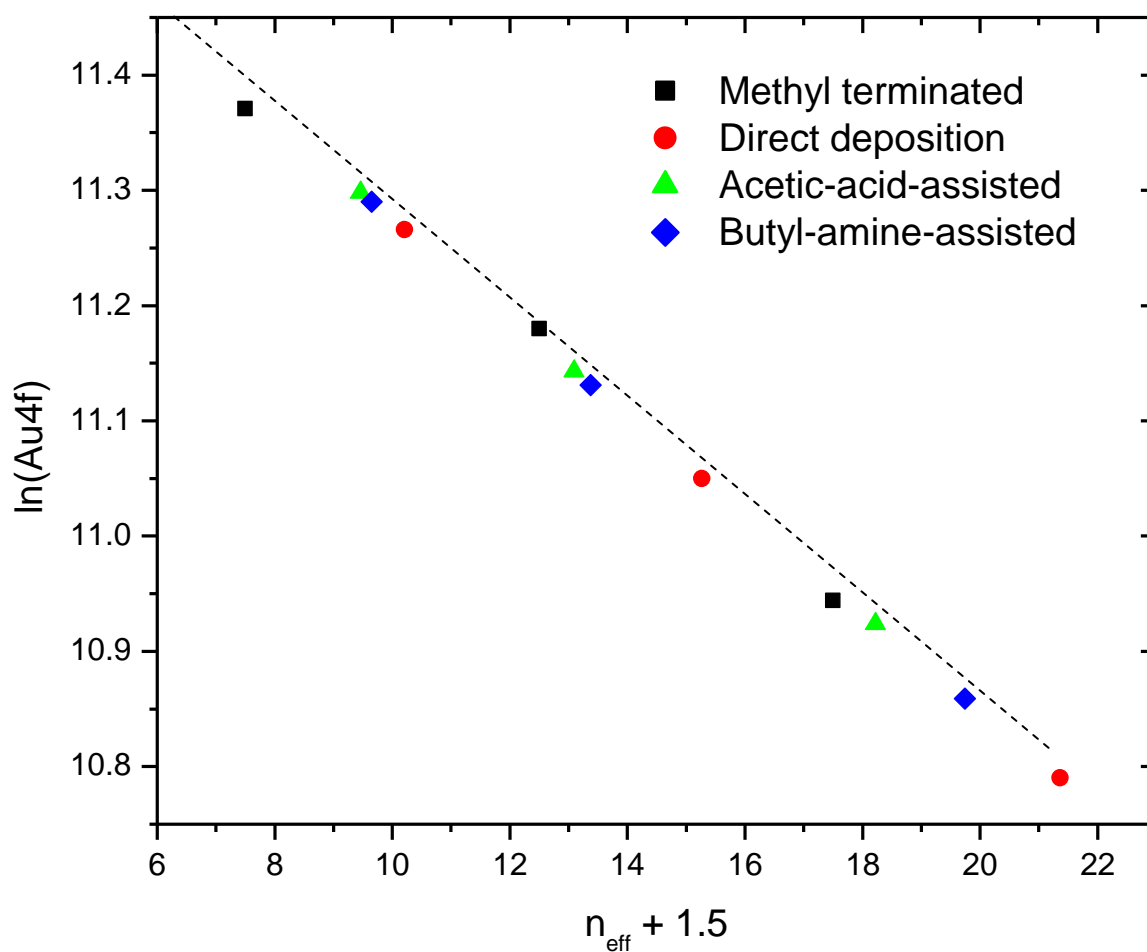9. H. Wang, S. Chen, L. Li and S. Jiang, *Langmuir*, 2005, **21**, 2633.

Fig. S1. Au4f attenuation as a function of the number of chain atoms in the molecule composing the SAM. The dashed line is a linear fit of the data for the methyl terminated system with n_{chain} set equal to n_{eff}. This linear fit is used as a calibration curve with the Au attenuation data for carboxylic acid terminated SAMs to determine those n_{eff} values.
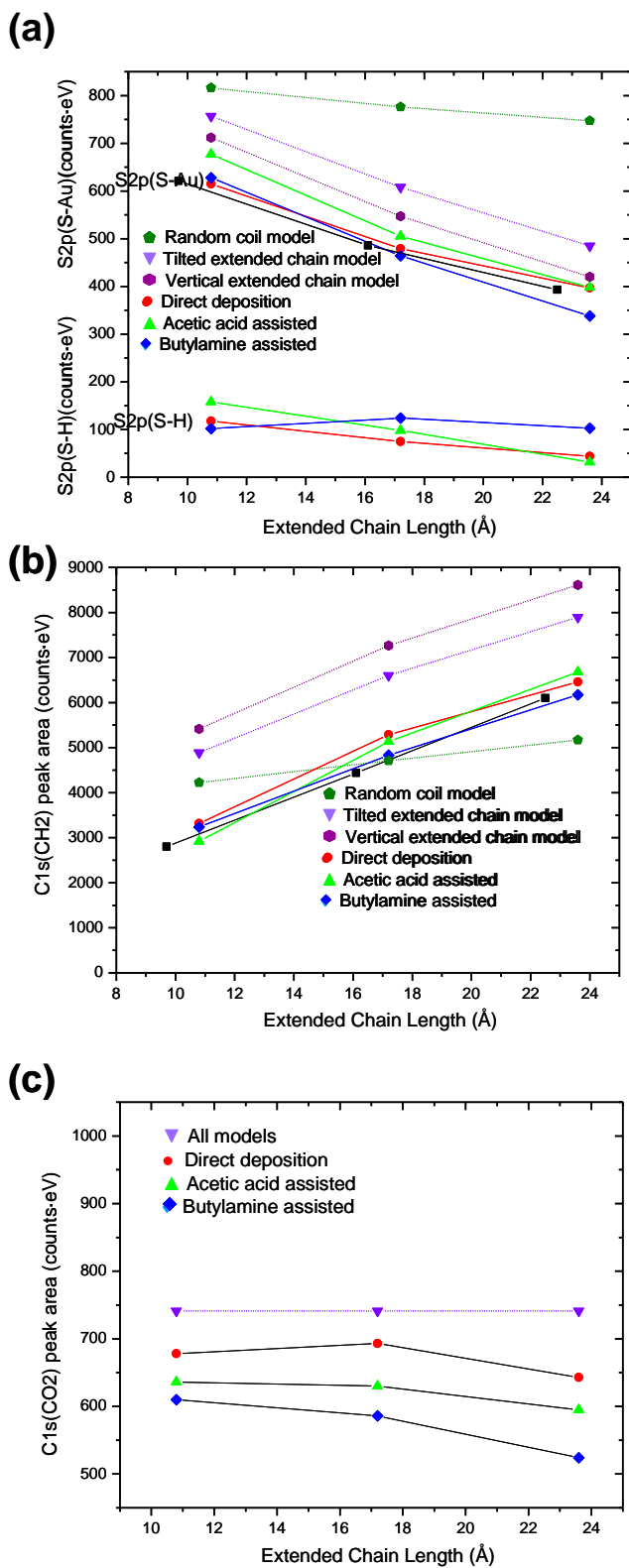
(a)

(b)

(c)

Fig. S2. Experimental and modeled XPS S2p (a), C1s (b). and (c) C1s(CO2) photoemission intensity as a function of methylene chain length for $HS(CH_2)_nCOOH$ SAMs deposited by direct, acetic-acid-assisted and butyl-amine-assisted procedures and calculated for the extended chain and random coil models.
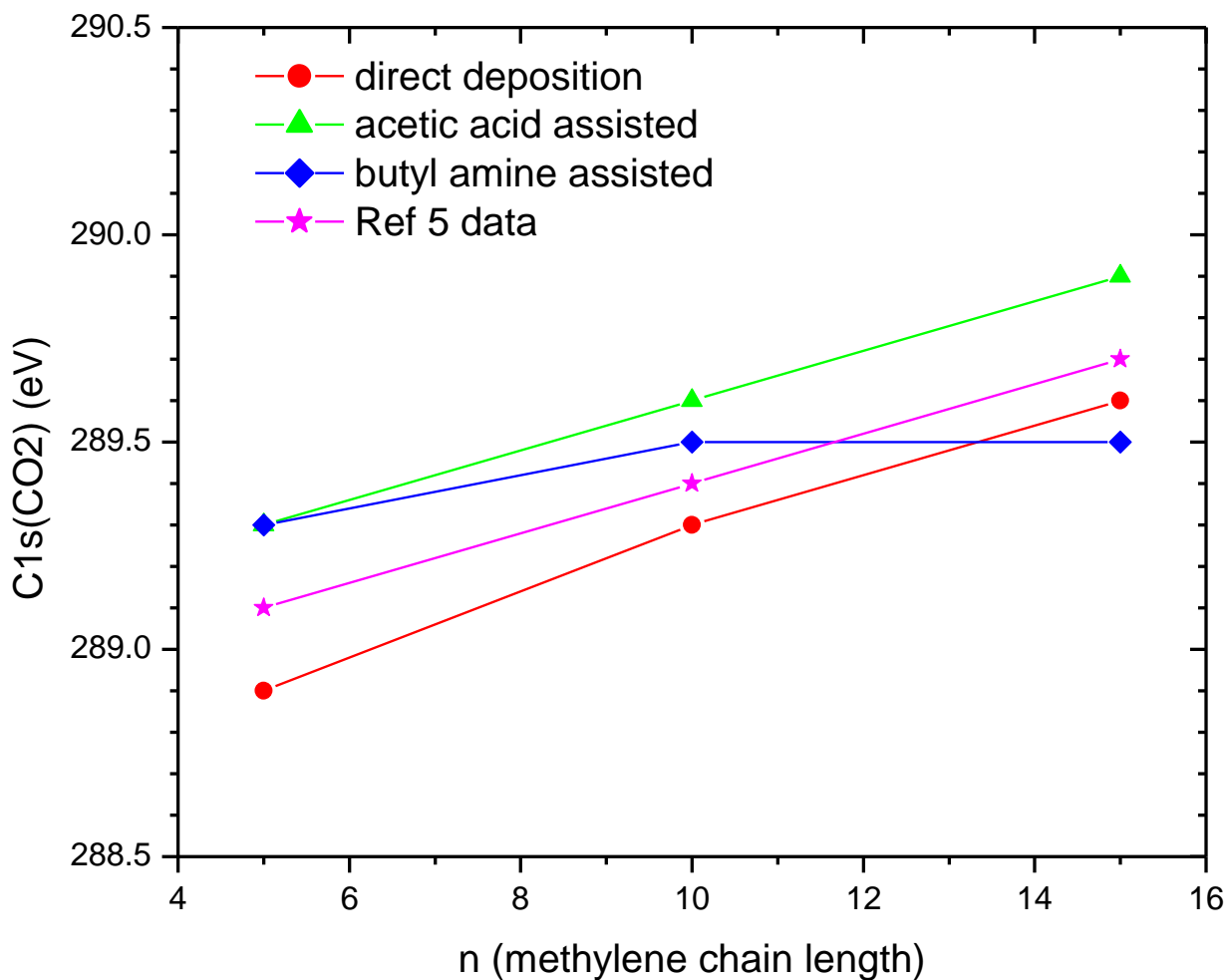
8

Fig. S3. Dependence of the $C1sCO_2$ emission peak maximum for the direct, acetic acid assisted, butyl amine assisted and from Techane et al[5] illustrating the anomalous dependence of the butyl-amine-assisted deposition.